A trio of unintended null experiments

An autobiographical indulgence
+
Why graduate students should not give up

Rainer Weiss, MIT

Louisiana State University

April 25, 2013

The experiments

- The fountain atomic clock
  - Paucity of slow atoms in a beam
  - A really precise clock with laser cooling
- The cosmic background as a velocity reference
  - The galactic interstellar dust got in the way
  - The right choices for COBE
- Tired light: cause for the Hubble expansion
  - QED works, photon/photon collisions do not
  - Experimental evidence for LIGO

Relevant properties of atomic clocks

- Single isolated quantum systems
  - Well defined states and energy levels
  - Each Cs atom the same as the next
  - Independent of epoch (maybe not?)
- Accuracy: anyone can set it up and get the same answer – control of systematics
- Precision: $\frac{\Delta f}{f} = \frac{1}{f \times t_{obs}} = \frac{1}{N_{cycles}}$ single atom

  $= \frac{1}{f \times t_{obs} \sqrt{n}}$ n atoms (no systematics)

Breit – Rabi plot Cs hfs energy vs B field

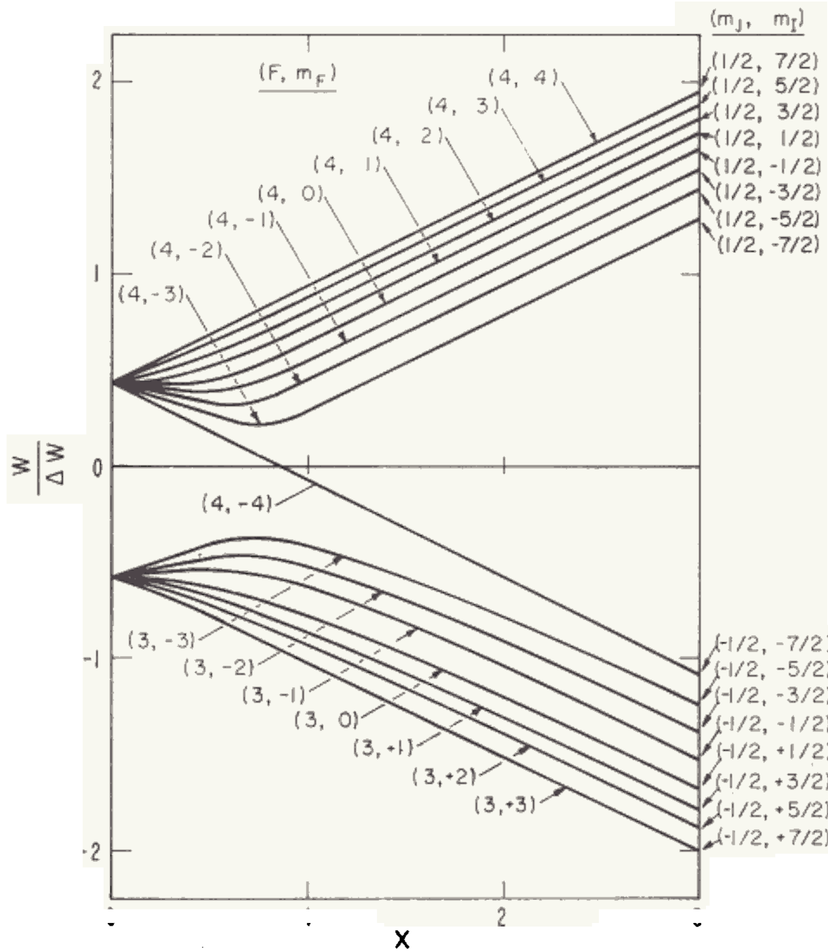

Fig. 1. Energy level diagram of Cs^{133} in the $^2S_{1/2}$ ground state as a function of the applied magnetic field

Rabi magnetic resonance apparatus

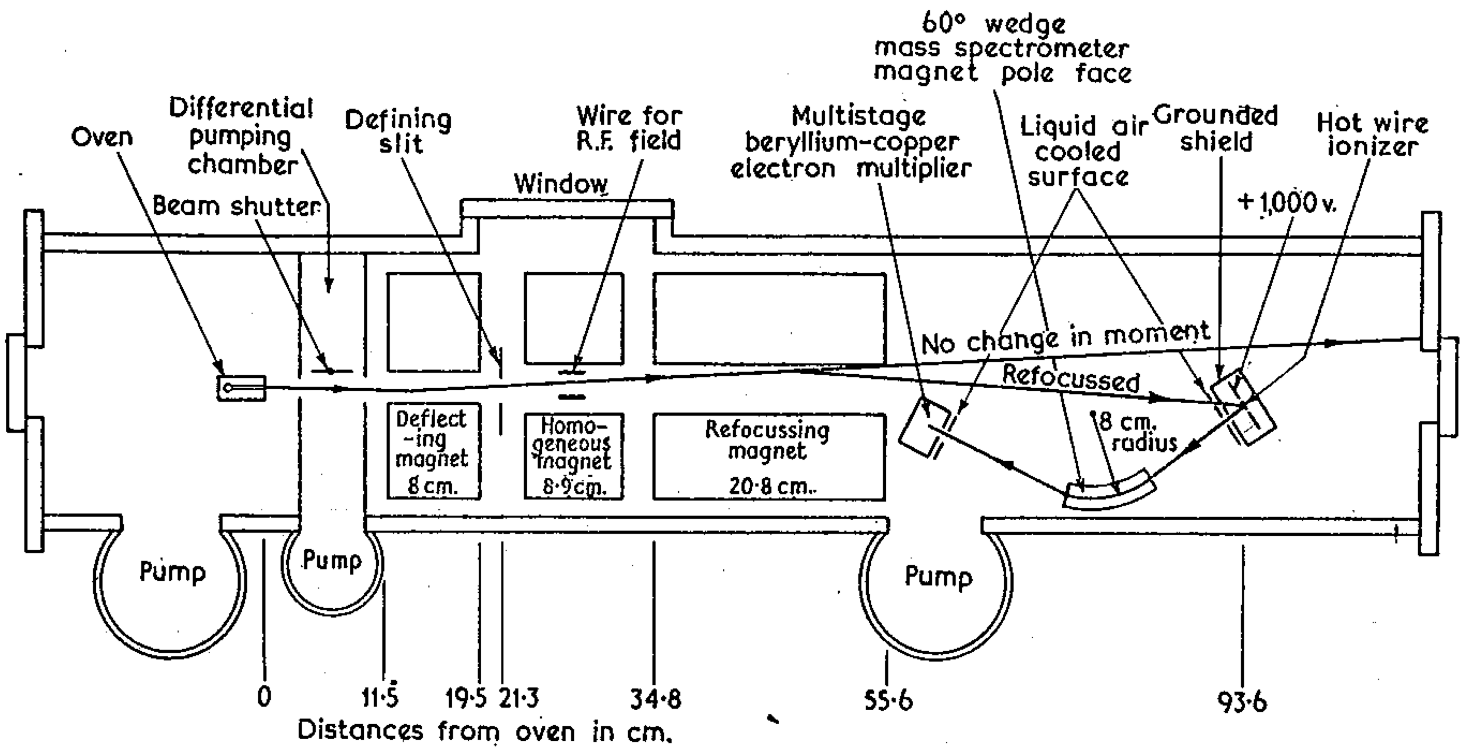

Small Cs clock

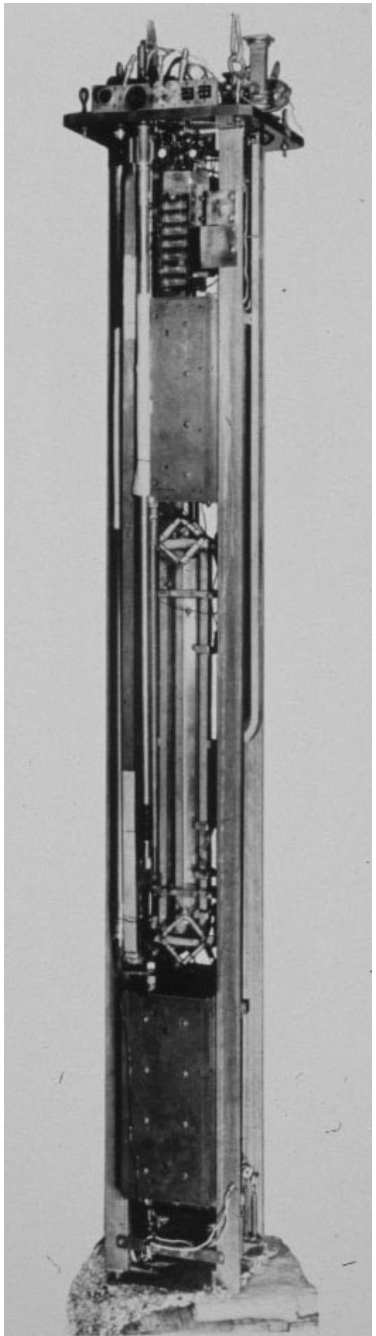

HE BOSTON HERALD, THURSDAY, JANUARY 27, 1955

MIT ATOMIC CLOCK ACCURATE

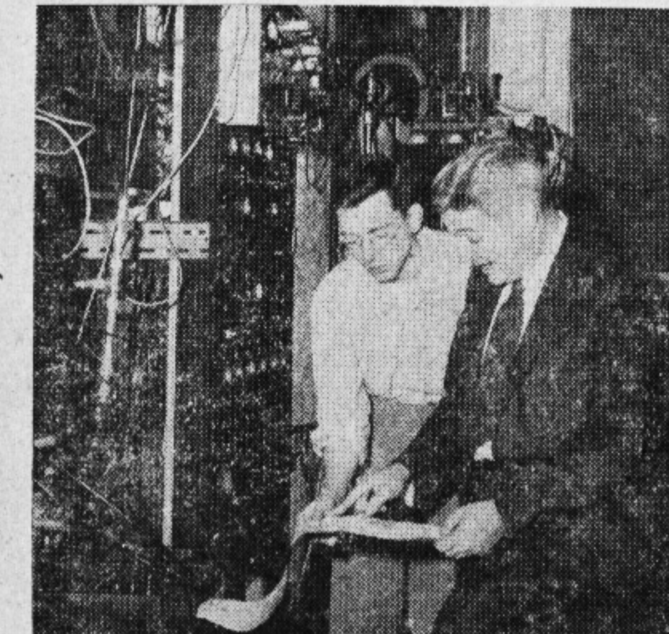

WORLD'S MOST ACCURATE CLOCK, an atomic timepiece developed at Massachusetts Institute of Technology, is examined by Robert D. Houn, Jr., graduate student, and Dr. Jerrold R. Zacharaias, director of the Laboratory for Nuclear Science.

An "atomic clock" which keeps good time that in 1955 years it would only be half a second off has been developed by scientiests of the Massachusetts Institute of Technology.

The clocks will be on the market withing ayear and the Malden manufacturer says they will range in price between $10,000 and $20,000.

MIT, always reserved in its announcements of discoveries, said that the atomic clock is "fantistically accurate" and "so precise that if it habd been ticking away since the time of Christ, it would now be only one - half second 'wrong.' "

TO TEST EINSTEIN

Development of the clock—the Cesium Atomic Frequency Standard—was announced yesterday by Dr. Jerrold R. Zacharias, director of the Laboratory for Nuclear Science at MIT.

He said the clock's primary use would be in scientific research, such as his own proposed testing of Einstein's General Theory of Relativity, but that the clock would also be invaluable in navigation, astronomy, geophysics and communication.

It is being manufactured by the National Company, 61 Sherman St., Malden.

'JUST BEGINNING'

Time-keeping in the device, Dr. Zacharias explains, is controlled by the oscillation of electrons in the cesium atom. Cesium is an elelment of the atomi cgroup which includes sodium and potassium and has a frequence of approximately 9192.632 megacycles per second.

It is this frequency htat serves as the unit of time in the atomic clock.

Standard time, the nuclear expert points out, is generally measured by the frequency of the oscillations of a crystal and is accurate to one prt in 10 to the ninth power.

But the atomic clock is accurate to one part in 10 to the 10th power or, 10,000,000,000.

Dr. Zacharias says, however, that such accuracy is "just the beginning" and that he expects to reach that on one part in 10 to the 12th power.

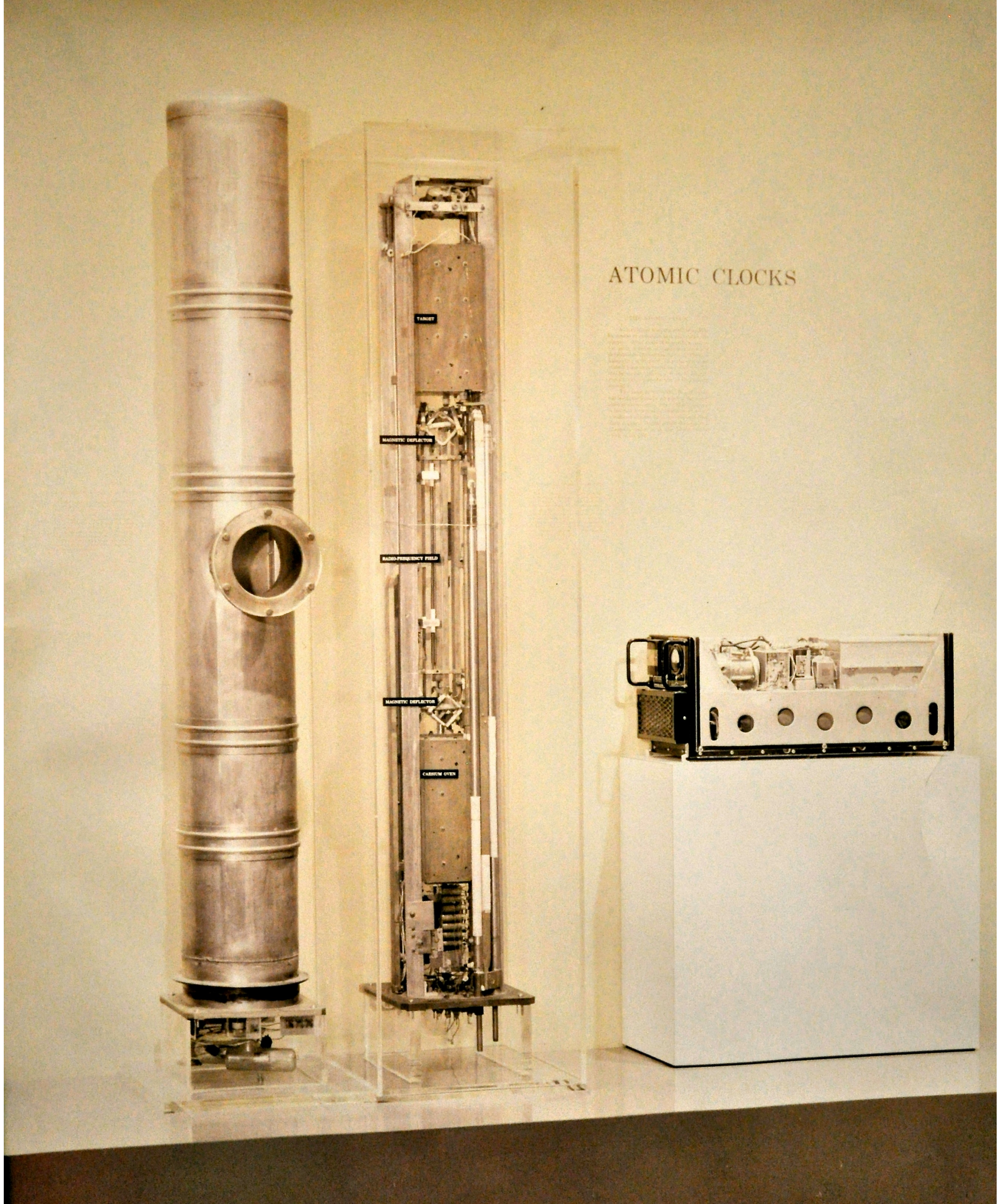
ATOMIC CLOCKS
TARGET
MAGNETIC DEFLECTOR
RADIO-FREQUENCY FIELD
MAGNETIC DEFLECTOR
CAESIUM OVEN

Ramsey separated oscillatory field excitation

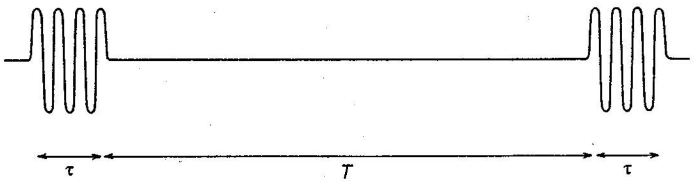

Fig. 4. Two separated oscillatory fields, each acting for a time τ, with a zero-amplitude oscillating field acting for time T. Phase coherency is preserved between the two oscillatory fields so it is as if the oscillation continued, but with zero amplitude, for time T.

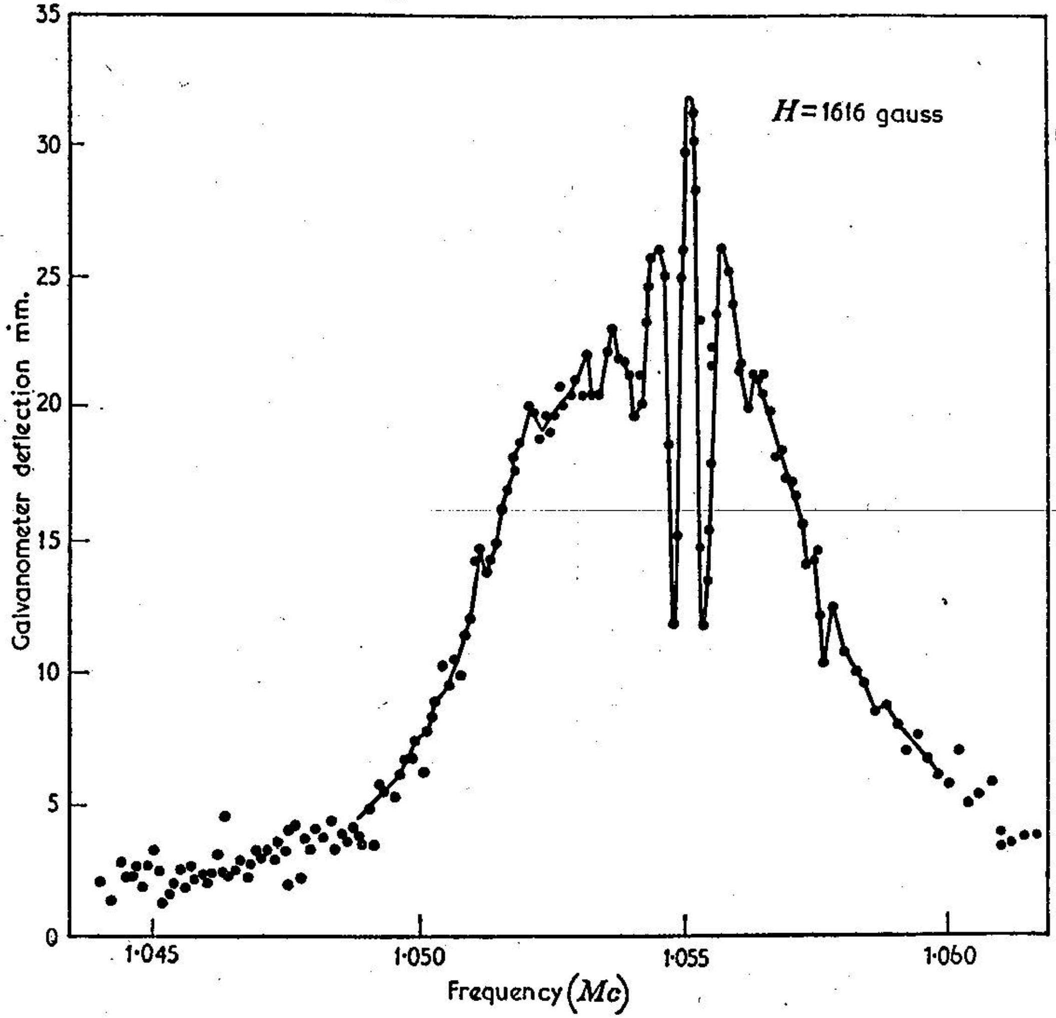

FIG. V. 4. Experimental transition probability for the central resonance of D_2 as a function of frequency with separated oscillating fields method (KOL 50a, KOL 52).

The Atomichron: National company

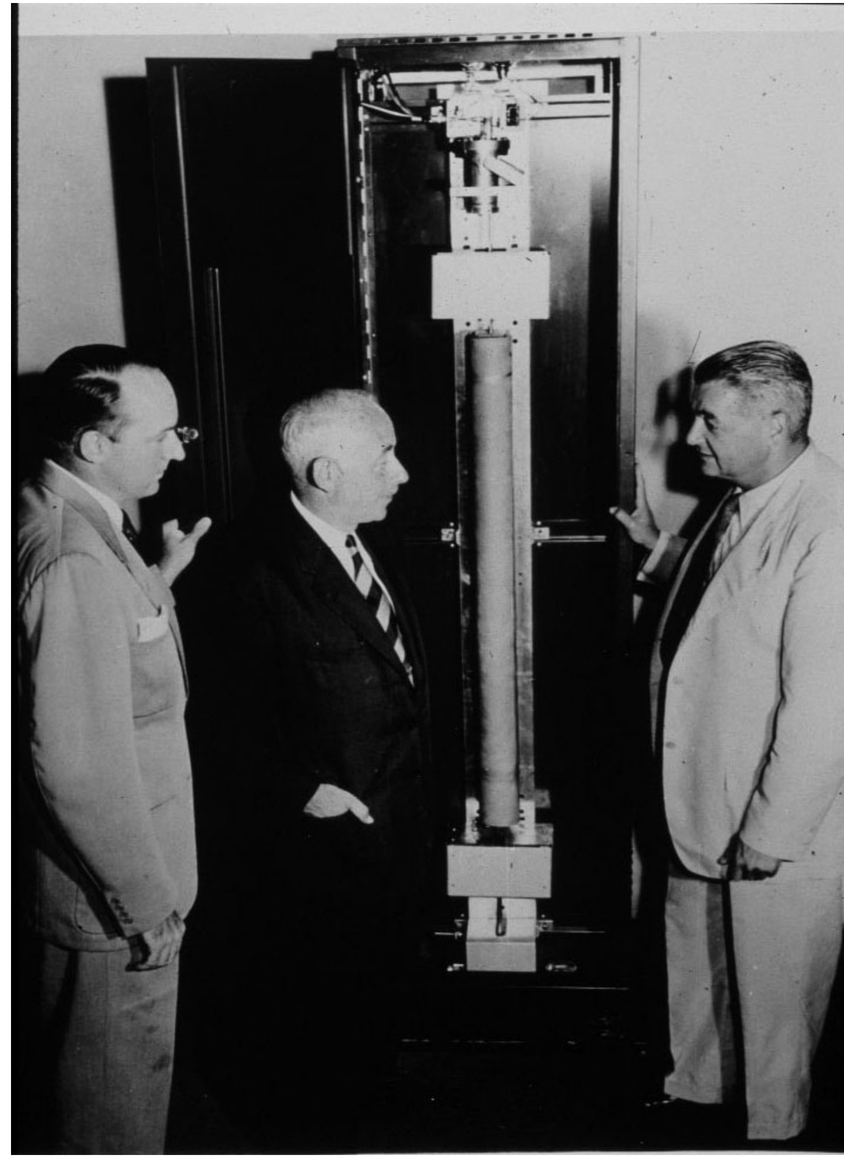

The big clock: Zacharias fountain

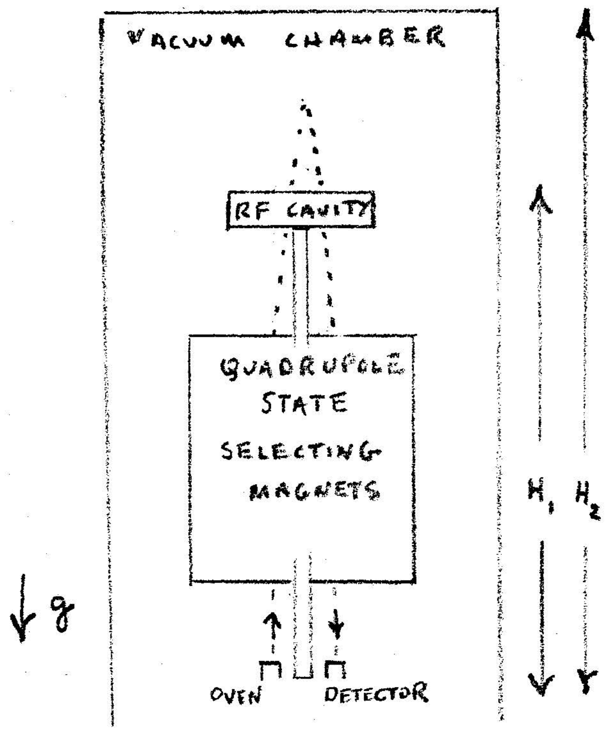

Figure 1.

$t_{observation} \sim 1 \sec$ $\frac{\Delta f}{f} \sim 10^{-10}$ per atom

Einstein red shift

$$\frac{\Delta f}{f} = \frac{gh}{c^2} = 5 \times 10^{-13} \text{ Jungfrau / valley}$$

Velocity of atoms in a beam

$$I(v) = \frac{2I_0 v^3}{\alpha^4} e^{-\frac{v^2}{\alpha^2}} dv \quad \alpha = \sqrt{\frac{2kT}{m}} \sim 2x10^4 \, cm/sec$$

Cs @ 373K

Beam intensity between two heights, $h/h_0 << 1$

$$I(h_2 - h_1) = \frac{I_0}{2h_0^2}\left(h_2^2 - h_1^2\right) \sim I_0 \times 2x10^{-6} \quad h_0 = \frac{\alpha^2}{2g} \sim 2.5km$$

h_2=5m h_1=3m

$\frac{v_2}{\alpha} \approx 1/22$

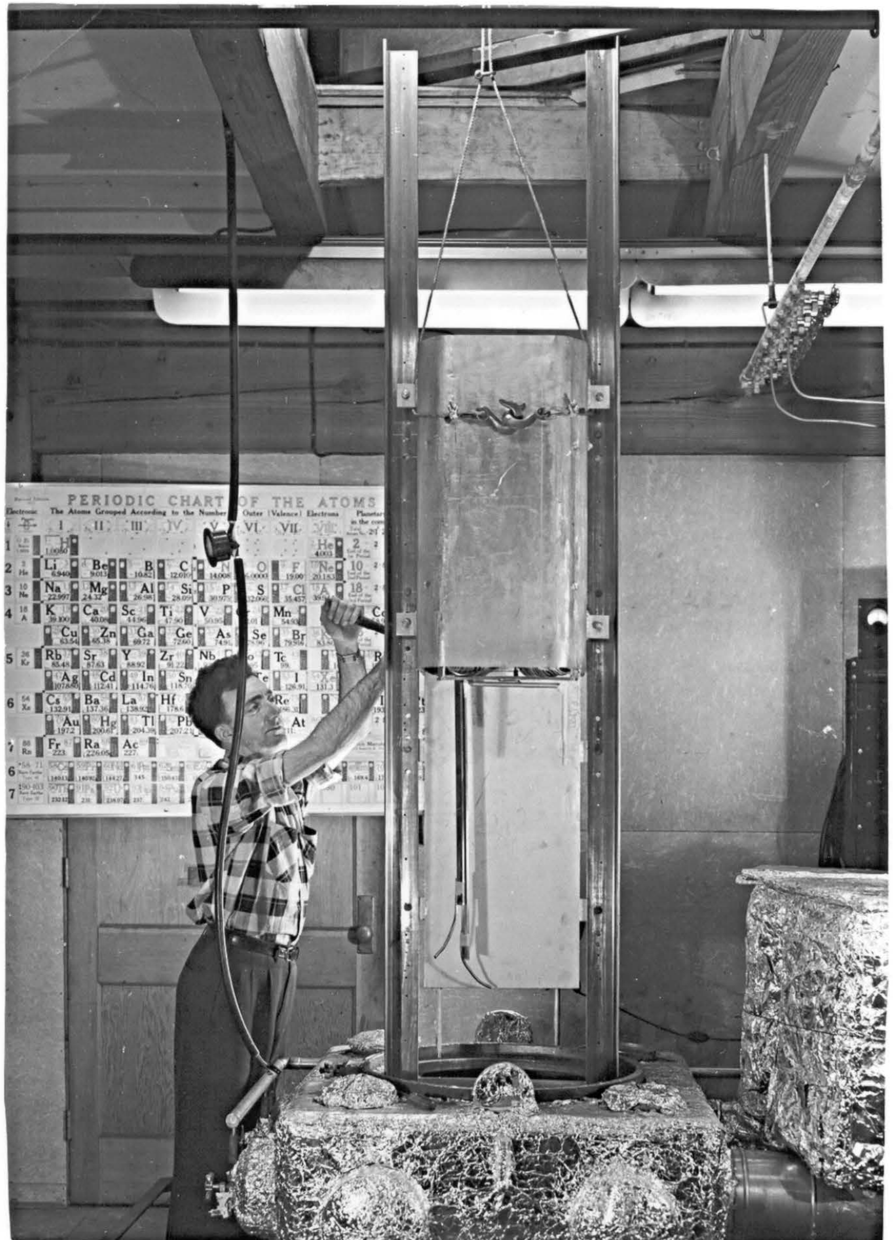

Frank O'Brien in 1956 adjusting the quadrupole deflecting magnets in the Zacharias fountain also called the "big clock" in the molecular beam lab at MIT.

Scaling for the fountain

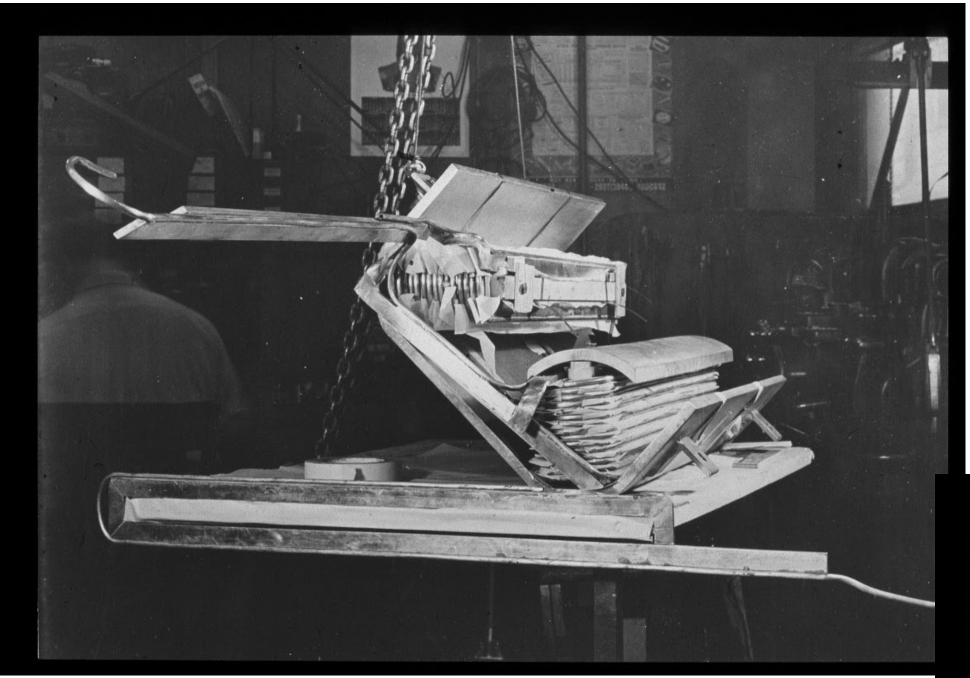

Gears to make corrugated sheet alternating with flat sheets for a multitube Cs oven

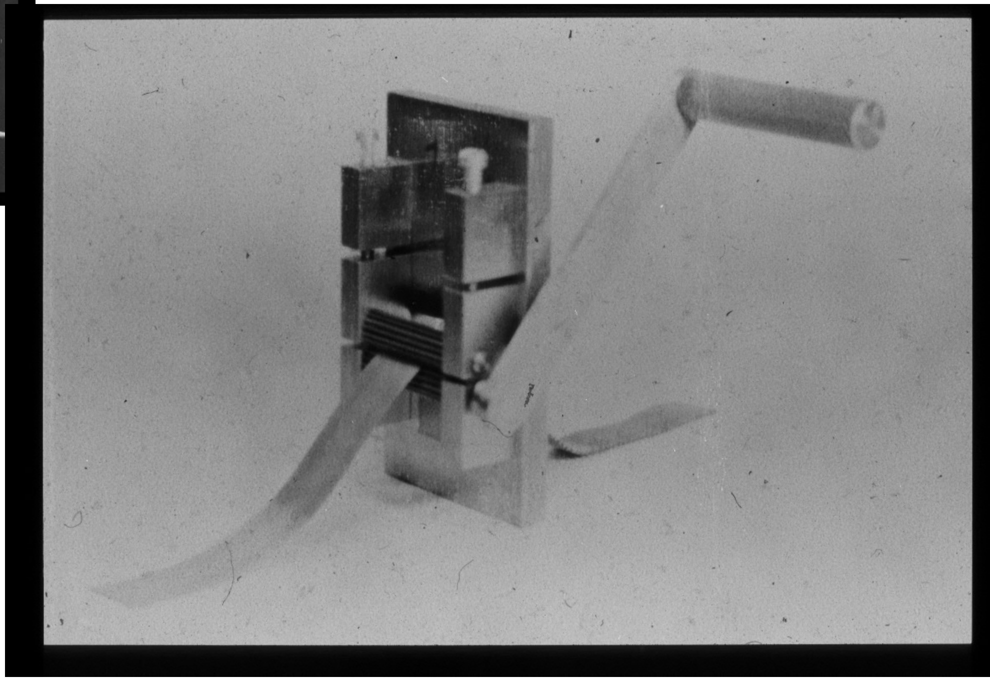

Quadrupole focusing magnet uses steel magnet image surface of structure for other poles

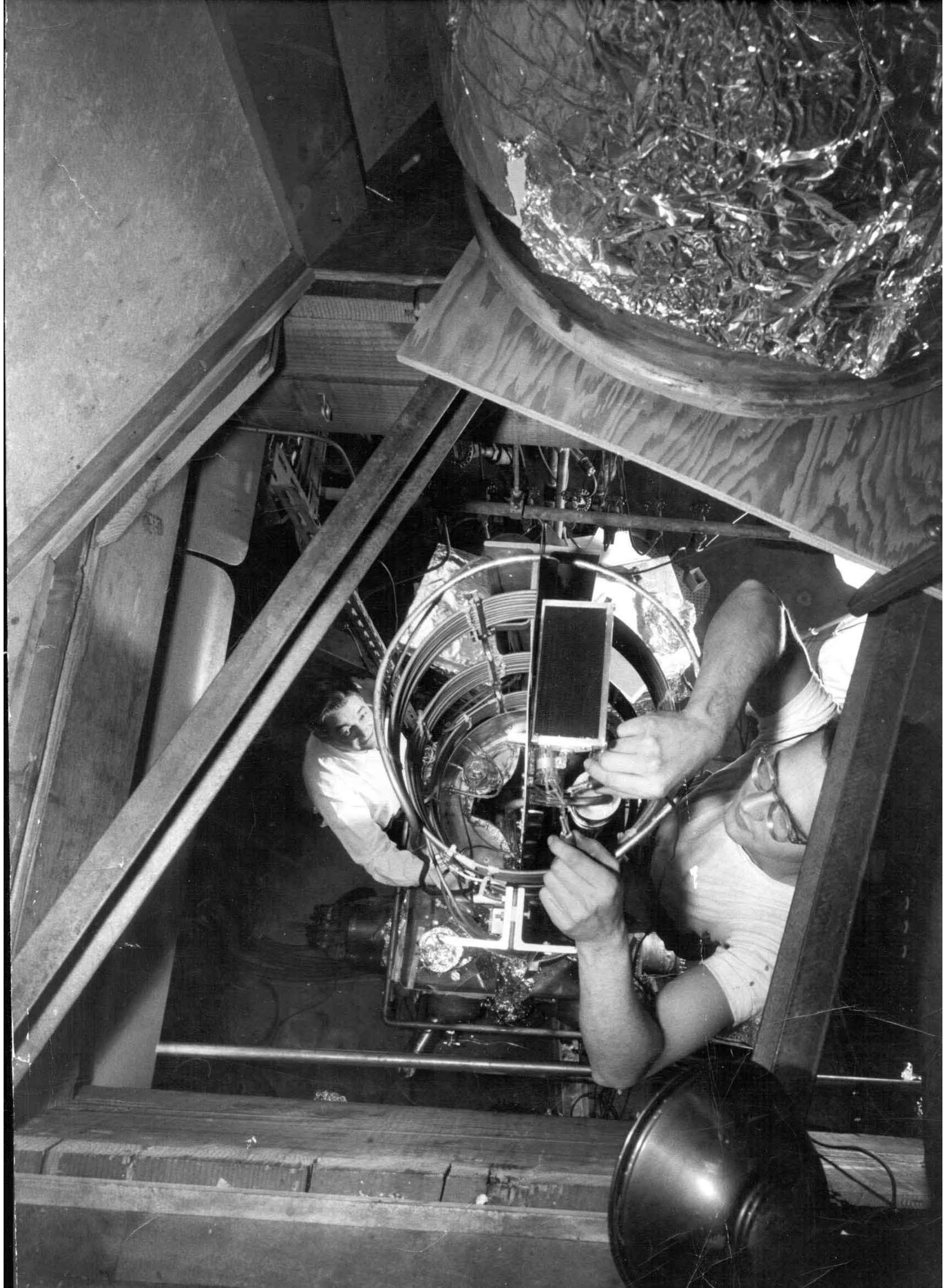

Pulse measurement of velocities

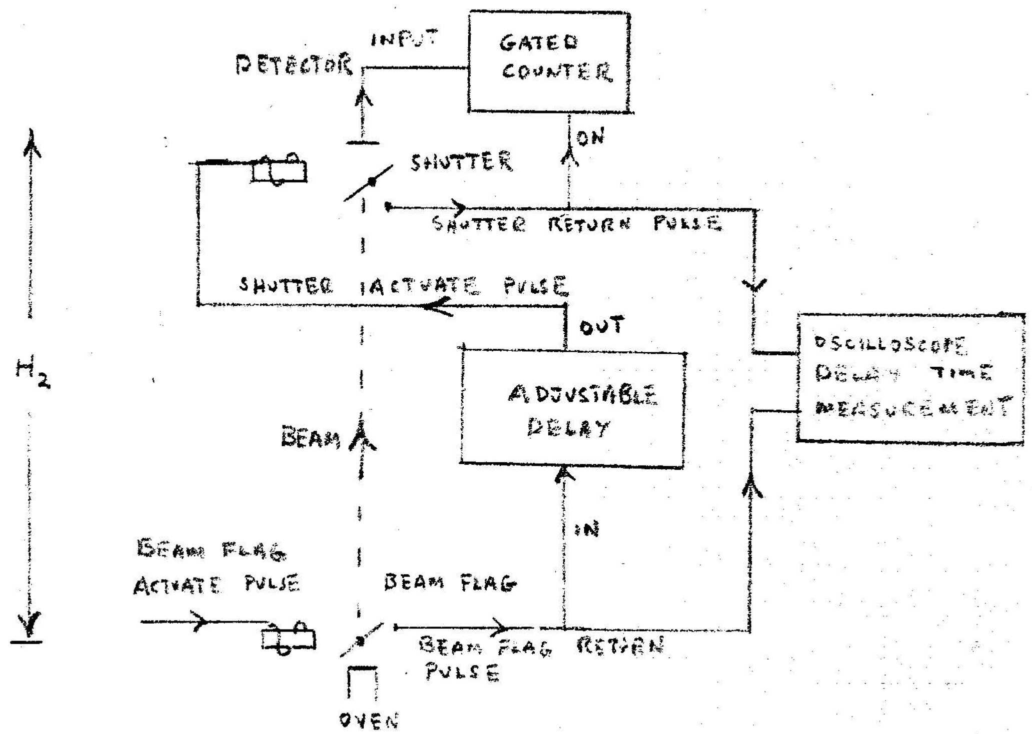

Apparatus had been extended through the next floor: h_2 = 6m, t_0=27 millisec

Big clock velocity data: what went wrong

Fast atoms scatter slow atoms in the beam

$$I_{detected} = 10^6 \text{ atoms / sec}$$

$$J_{oven} = 3\text{x}10^{14} \text{ atoms / sec/ cm}^2$$

$$Q_{Cs/Cs} = 2\text{x}10^{-13} \text{cm}^2$$

60 hits/slow atom for t/t_0=22

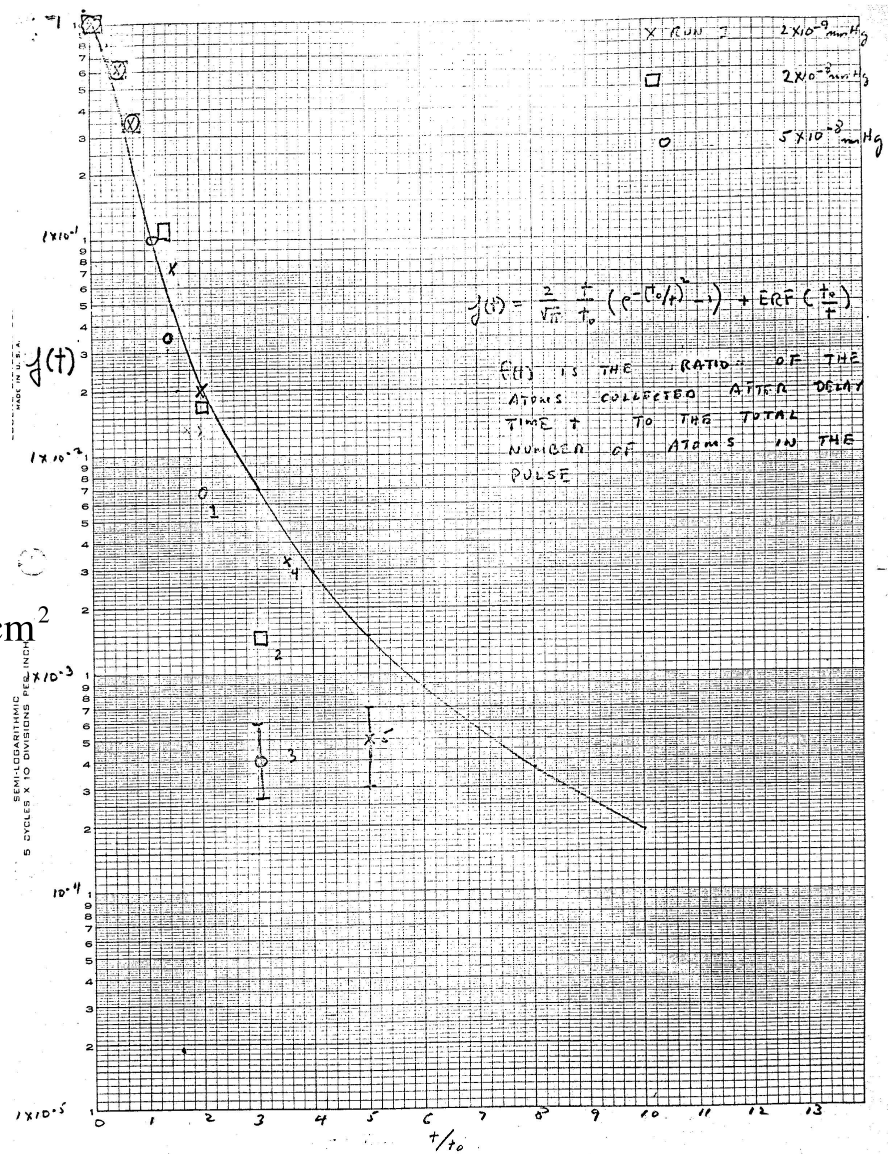

Zacharias Fountain 1991

EUROPHYSICS LETTERS 7 September 1991

Europhys. Lett., **16** (2), pp. 165-170 (1991)

Ramsey Resonance in a Zacharias Fountain.

A. CLAIRON (*), C. SALOMON (**), S. GUELLATI (***) and W. D. PHILLIPS (*$_*$*)

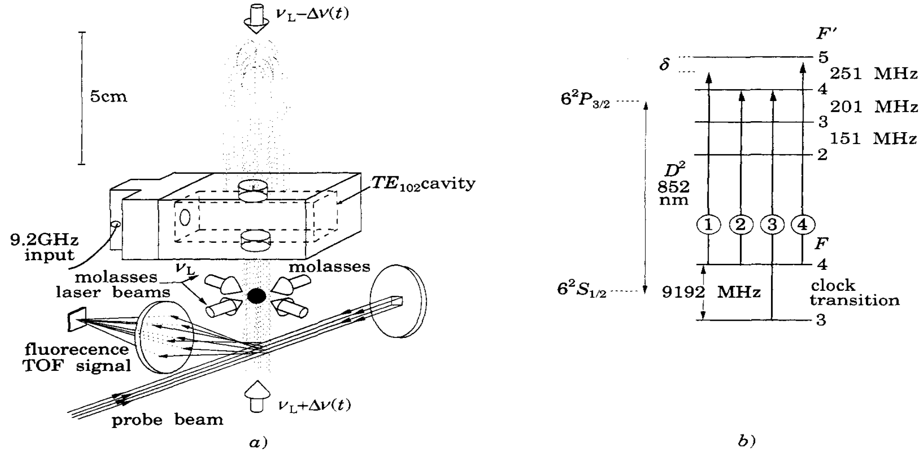

Fig. 1. – *a*) The Zacharias-style fountain. Cs atoms at 5.5 μK are launched from a «moving» molasses through a microwave cavity. The change of hyperfine state, due to the Ramsey resonance after passing twice through the cavity, is detected by state-selective resonance fluorescence in the probe beam. *b*) Relevant Cs transitions. Molasses loading and launching: 1 + 3. Hyperfine pumping: 2. Detection: 4.

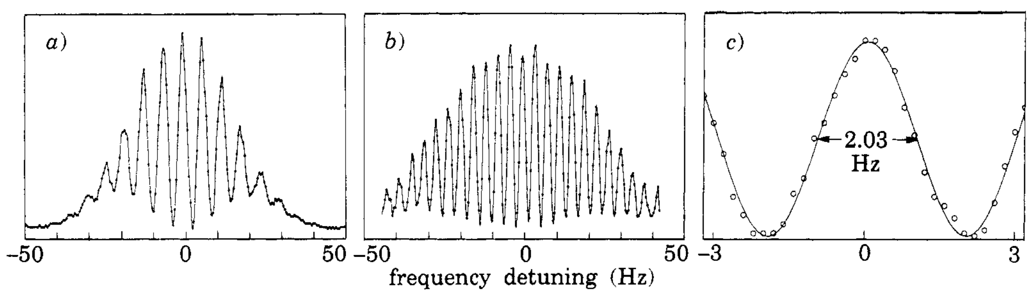

Fig. 2. – Ramsey fringes for two launch conditions. Each dot is the average of 5 fountain cycles. *a*) $v_z = 1.19$ m/s, $T = 26$ μK. Atoms reach 3.4 cm above the cavity for a 3.0 Hz wide fringe. Frequency step: 0.5 Hz. *b*) $v_z = 1.41$ m/s, $T = (5.5 \pm 1)$ μK. Fringe width 2.0 Hz. *c*) Central fringe of *b*) at 0.2 Hz frequency step. The curve is a least-square fit to a cosine lineshape. The standard deviation is 2.8%. The frequency standard deviation is 50 mHz and is dominated by the instability of the 9.2 GHz source.

Cosmic Background as velocity reference

- Critical issues after discovery of the Cosmic Background
  - Is the spectrum thermal – a Planck distribution in frequency
  - Is the angular distribution isotropic

Spectrum

$$B(f,T)df = \frac{2hf^3}{c^2}\left(\frac{1}{e^{\frac{hf}{kT}}-1}\right)df$$

$$B(\upsilon,T)d\upsilon = \frac{1.19x10^{-12}\upsilon^3 d\upsilon}{e^{\frac{1.44\upsilon}{T}}-1}$$ w/cm²/sr

Peak in wavenumbers at 2T

Anisotropy due to motion of detector relative to last scatterers

$$T(\theta) = \frac{T_0\sqrt{(1-\frac{v^2}{c^2})}}{1-\frac{v}{c}\cos(\theta)}$$

Best estimate in 1970's : v/c = 1 x 10^{-3}
due to rotation of our galaxy

Spectrum 1972 - 1978

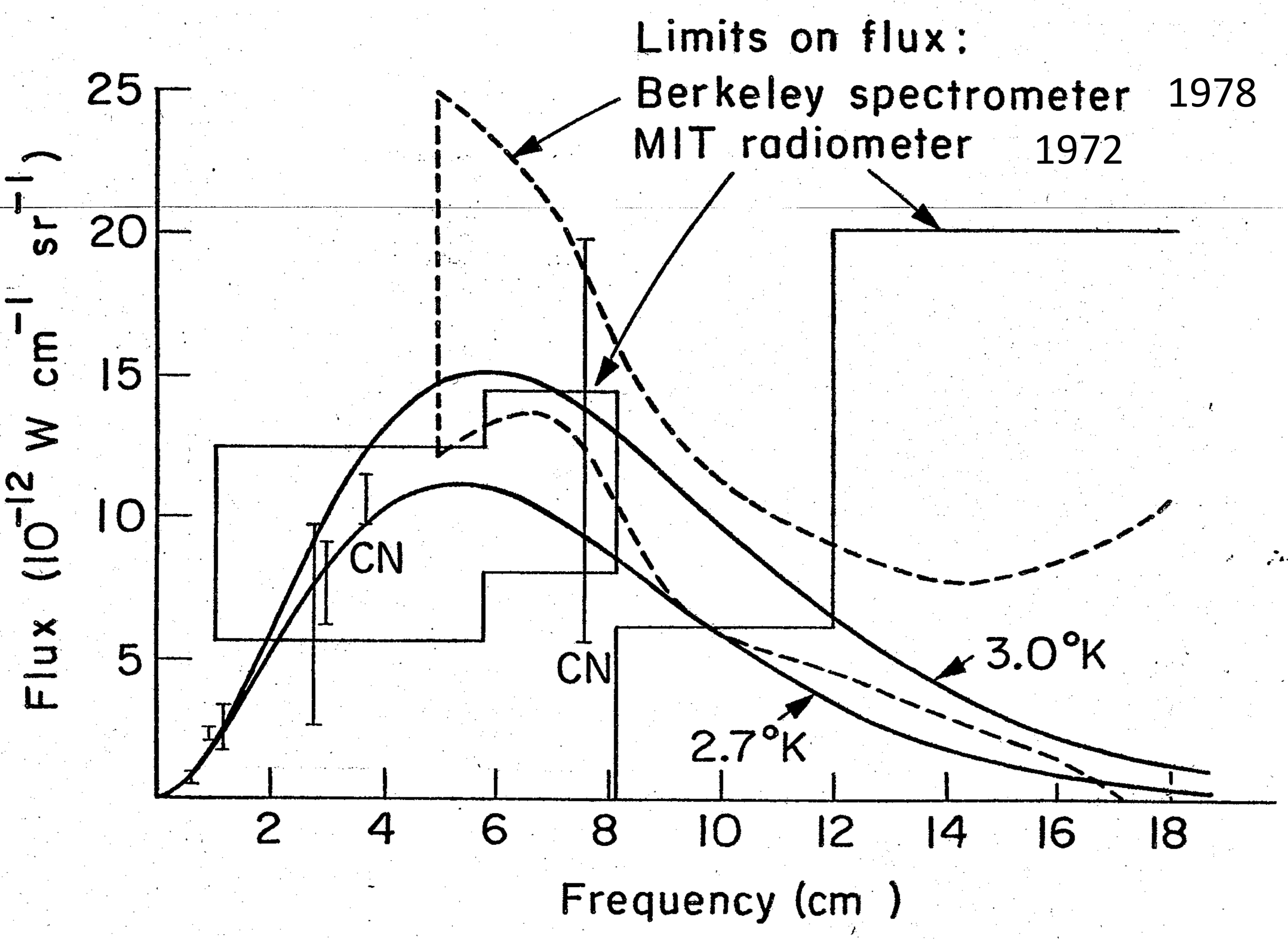

D.Muehlner

MIT anisotropy instrument

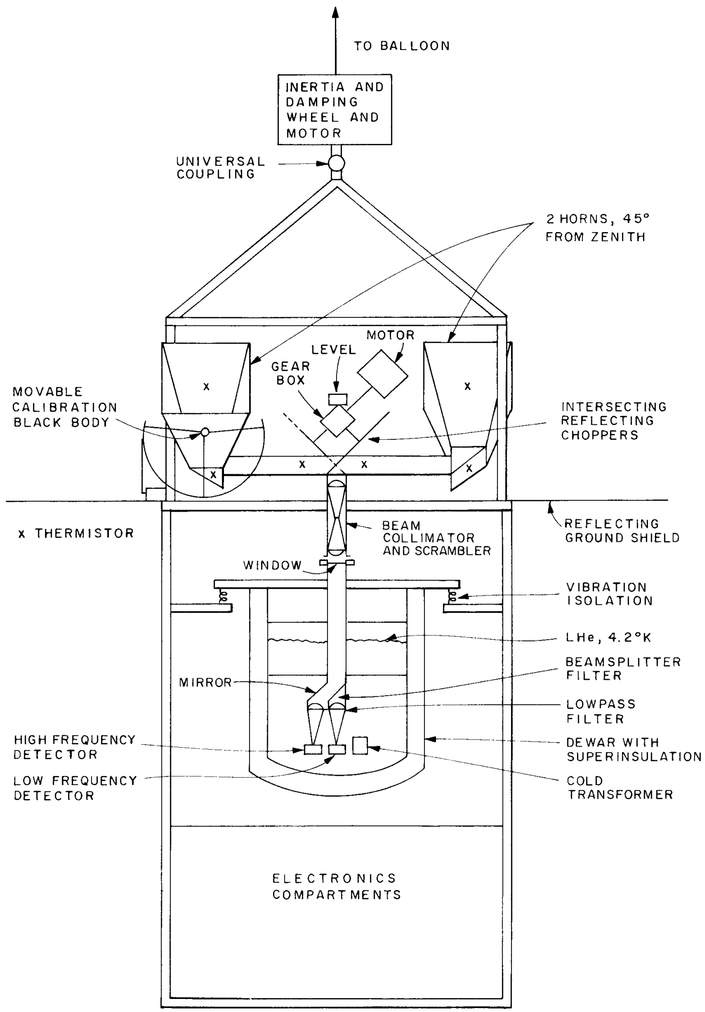

Fig. VI-1. The apparatus.

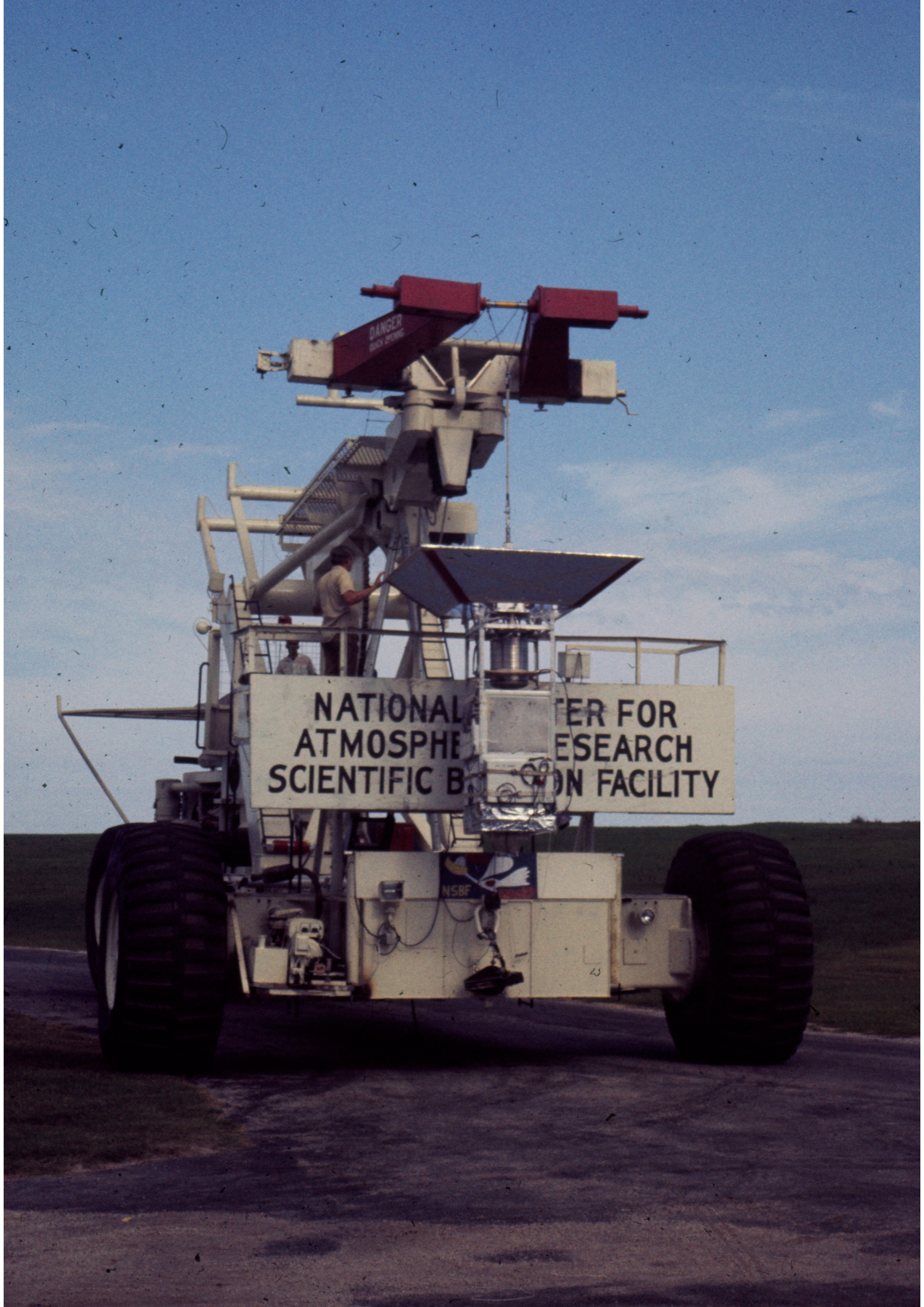
DANGER
NATIONAL TER FOR
ATMOSPHE ESEARCH
SCIENTIFIC B ON FACILITY
NSBF



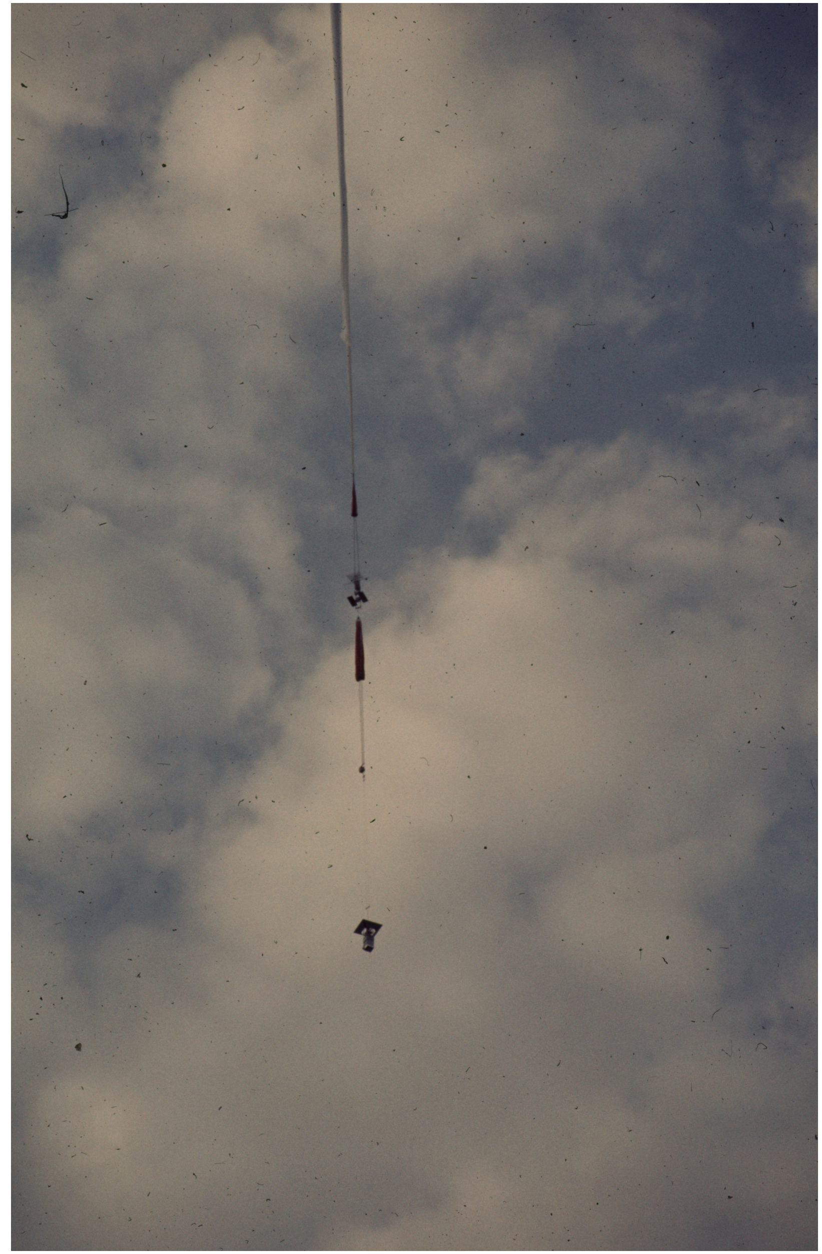

Moon seen in anisotropy instrument

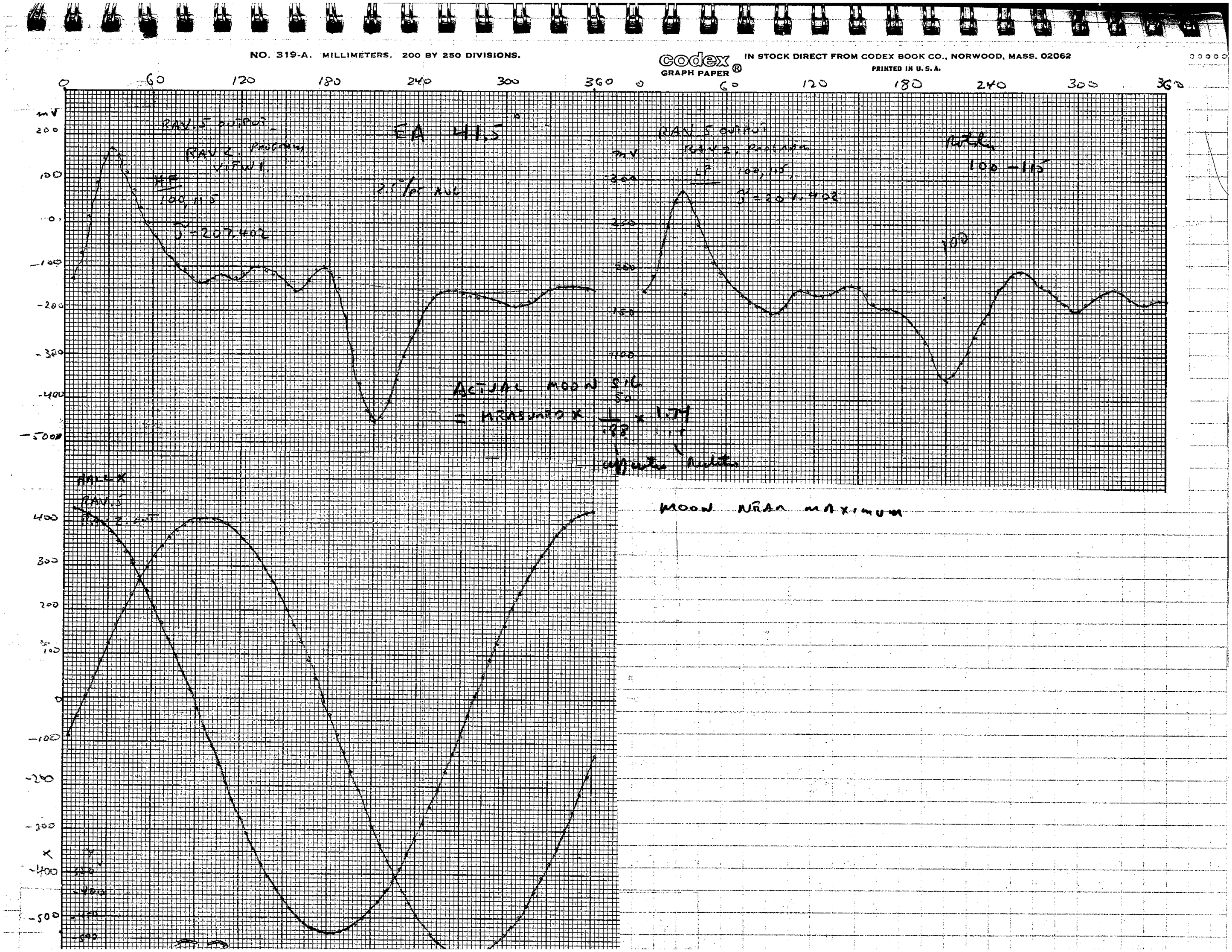

First look and the disaster

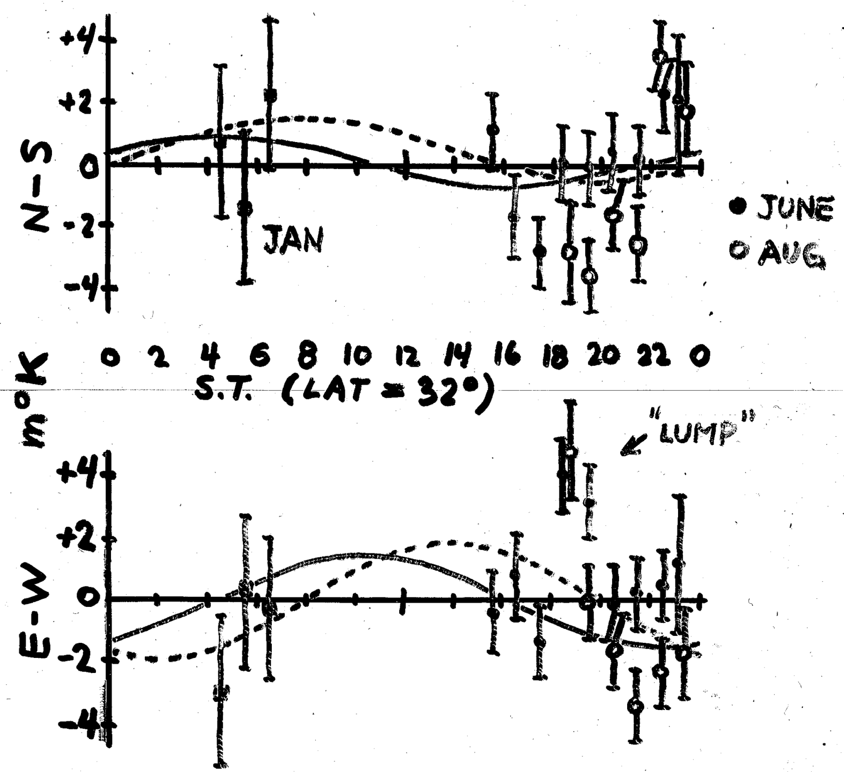

MIT Submm. ISOTROPY DATA

1974 Balloon Flights

$$\Delta T \cong T_0 \left(1 + \frac{v}{c} \cos\theta\right)$$

Small beam anisotropy instrument

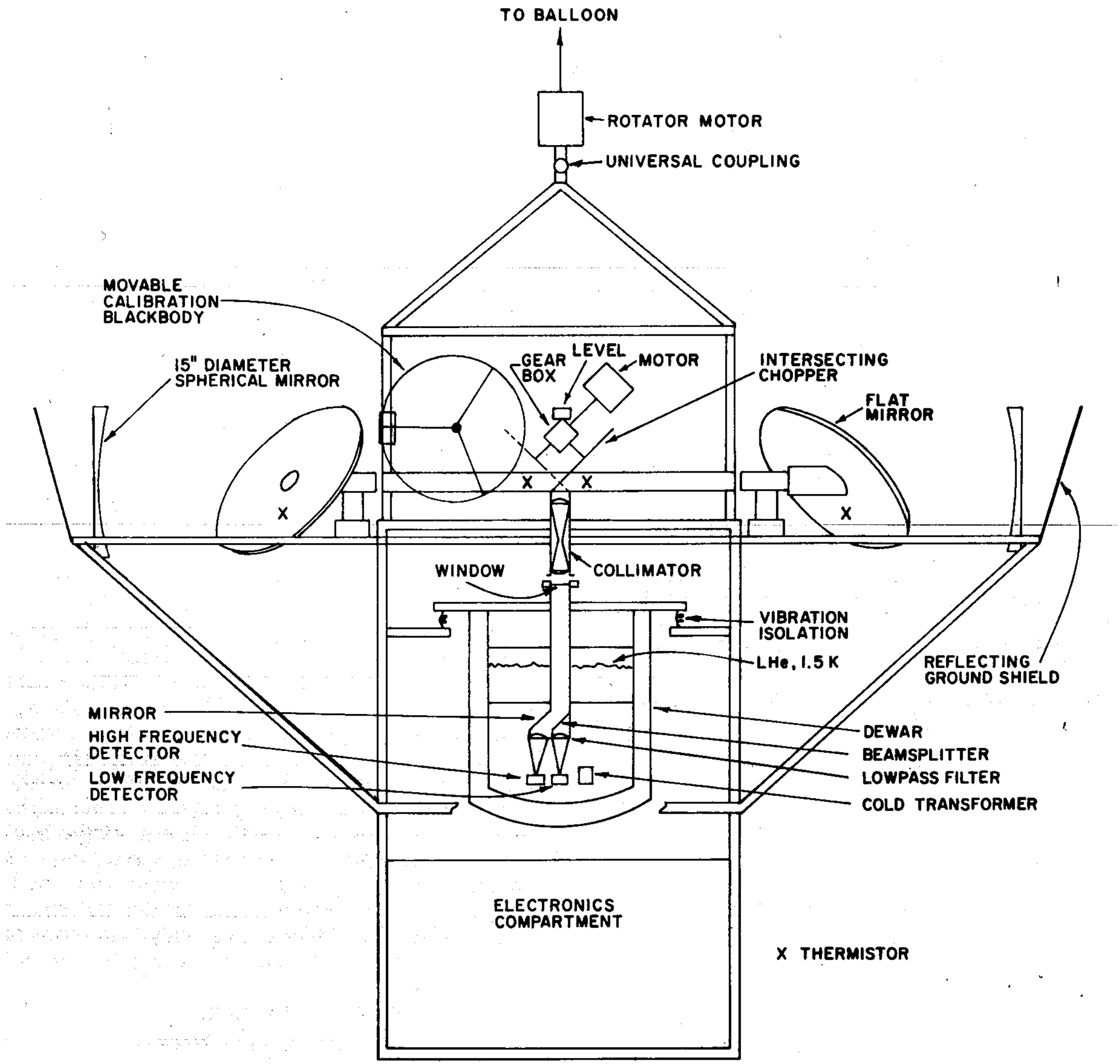

Small beam results

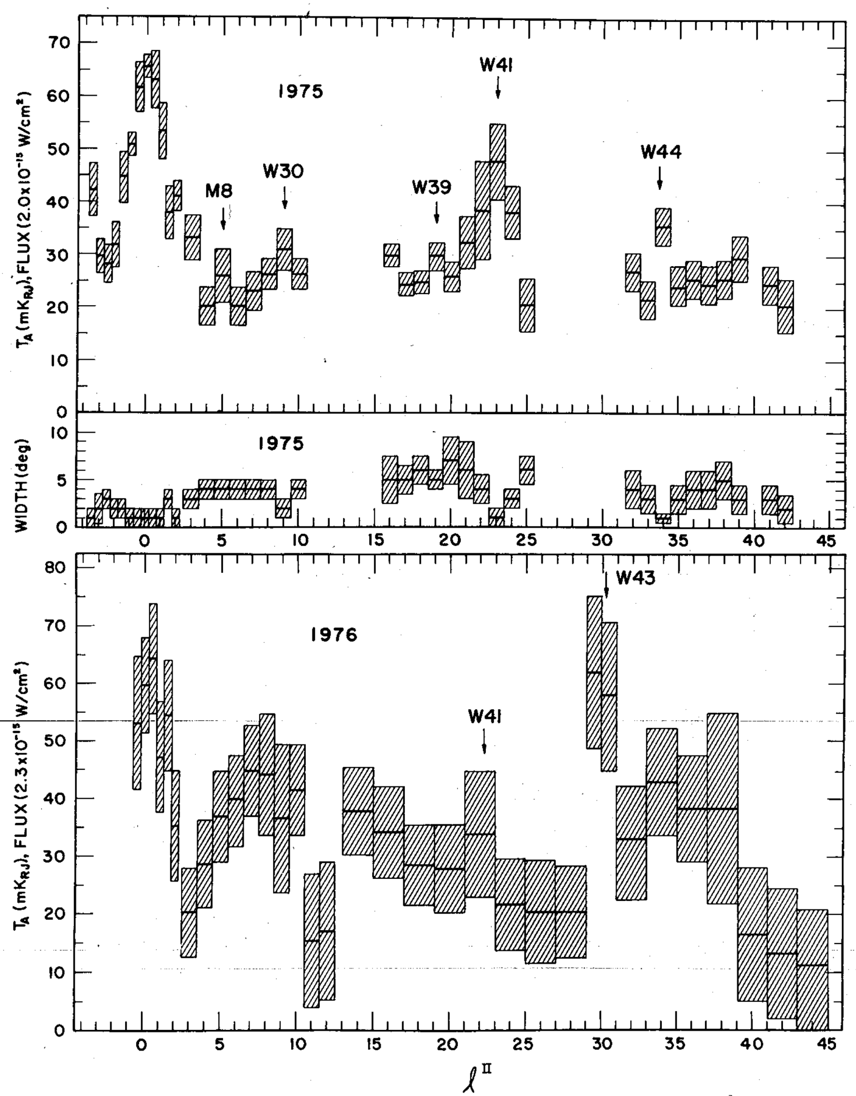

FIG. 5.—Galactic disk as measured in both flights. *Upper graph*, 1975 flight. The upper curve in the graph presents the equivalent antenna temperature of the disk as a function of galactic longitude, $b^{II} \approx 0$. The lower curve shows the half-power widths of the disk. *Lower graph*, 1976 flight. The locations in l^{II} of several known radio sources are shown. The vertical extent of a shaded rectangle represents error bars, and the horizontal extent covers the region of l^{II} which was averaged together. The entire detecting system in the 1976 flight was a.c.-coupled restricting full response to sources less than 3° in width, and no attempt was made to measure the width of the disk.

D.K.Owens

Galactic map of 30 cm^{-1} data

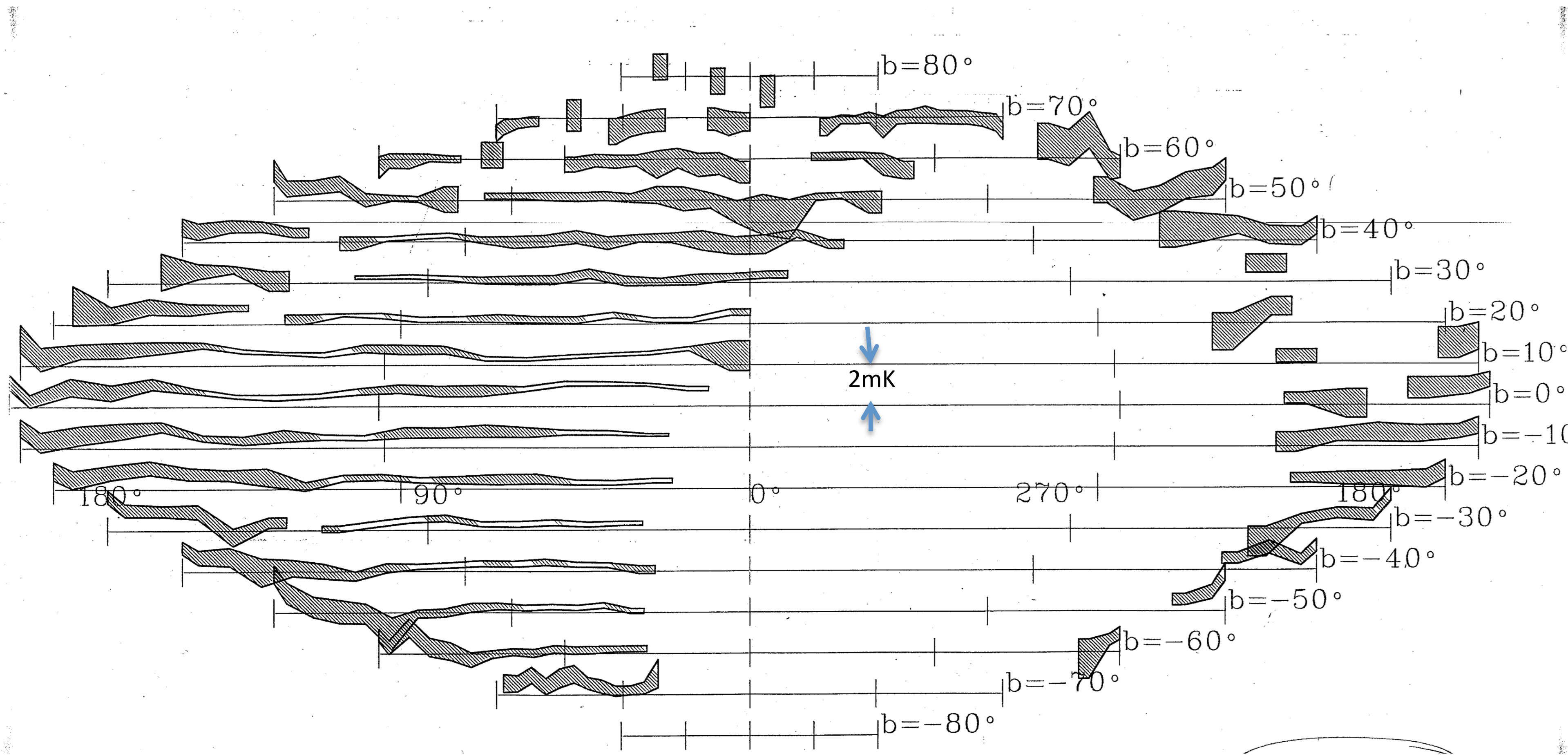

M. Halpern

Dipole after much turmoil

TABLE 9

MEASUREMENTS OF A DIPOLE ANISOTROPY IN THE CBR

Author	λ (cm)	ΔT_{Ant} (mK_{RJ})	ΔT_{CBR}[a] ($mK_{thermo.}$)	R.A. (hr)	δ (°)
Partridge and Wilkinson 1967	3.20	0.9 ± 2.1	0.9 ± 2.1	...	...
Conklin 1969	3.75	1.6 ± 0.8	1.6 ± 0.8	...	...
Boughn, Fram, and Partridge 1971	0.86	7.3 ± 11.2	7.5 ± 11.6	...	...
Smoot and Lublin 1979	0.91	3.01 ± 0.39	3.1 ± 0.4	11.4 ± 0.4	9.6 ± 6.0
Boughn, Cheng, and Wilkinson 1981	1.58	2.97 ± 0.79	3.0 ± 0.8	12.0 ± 1.3	$-18. \pm 18.$
	1.21	3.94 ± 0.30	4.0 ± 0.3	11.6 ± 0.3	$-2. \pm 3.$
	0.95	3.61 ± 0.29	3.7 ± 0.3	11.0 ± 0.3	$-8. \pm 4.$
	0.65	3.69 ± 0.95	3.9 ± 1.0	11.6 ± 0.9	$-12. \pm 14.$
Fixsen, Cheng, and Wilkinson 1983	1.22	3.13 ± 0.167	3.17 ± 0.17	11.08 ± 0.04	-8.1 ± 0.62
Lubin, Epstein, and Smoot 1983	0.33	2.79 ± 0.138	3.42 ± 0.17	11.2 ± 0.1	$-6. \pm 1.5$
This Work					
Channel 1	0.17	1.53 ± 0.194	3.40 ± 0.42	12.1 ± 0.24	$-23. \pm 5.$
Channel 2	0.08	0.364 ± 0.105	4.7 ± 1.4	$9.9^{+1.7}_{-1.1}$	$-38. \pm 21.$

[a] Thermodynamic temperature shift assuming $T_{CBR} = 2.74$ K.

Astrophysical Foregrounds

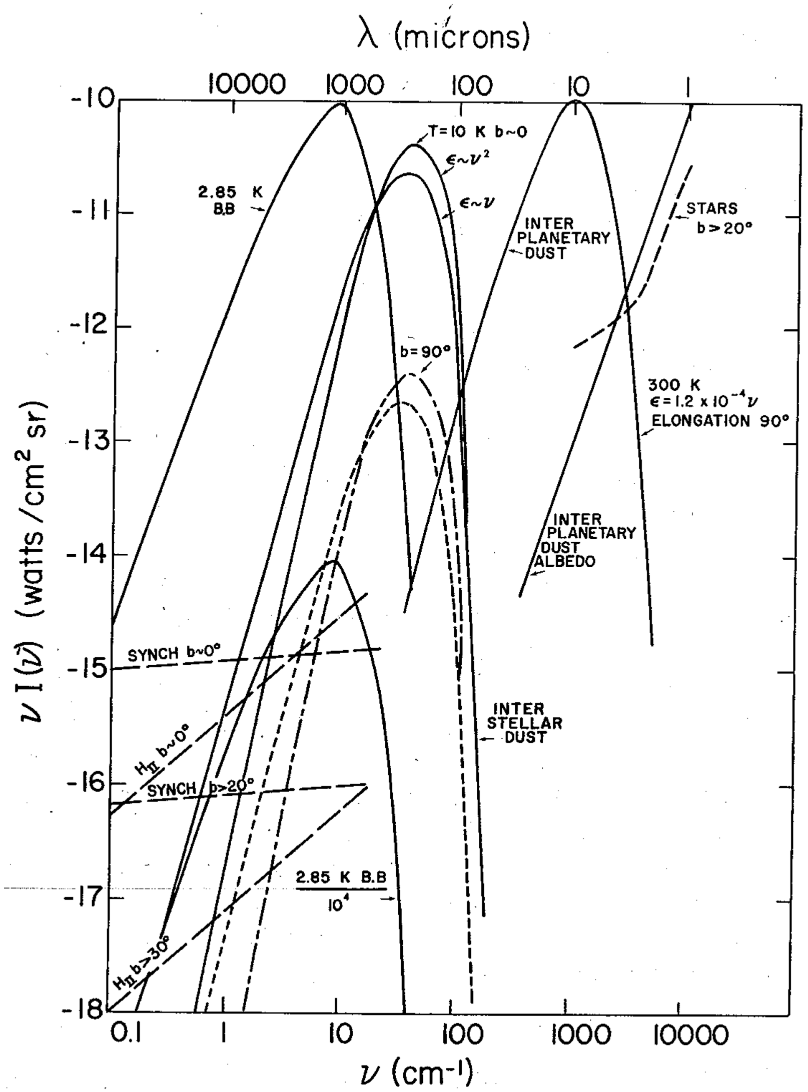

Figure 3 The astrophysical background.

COBE

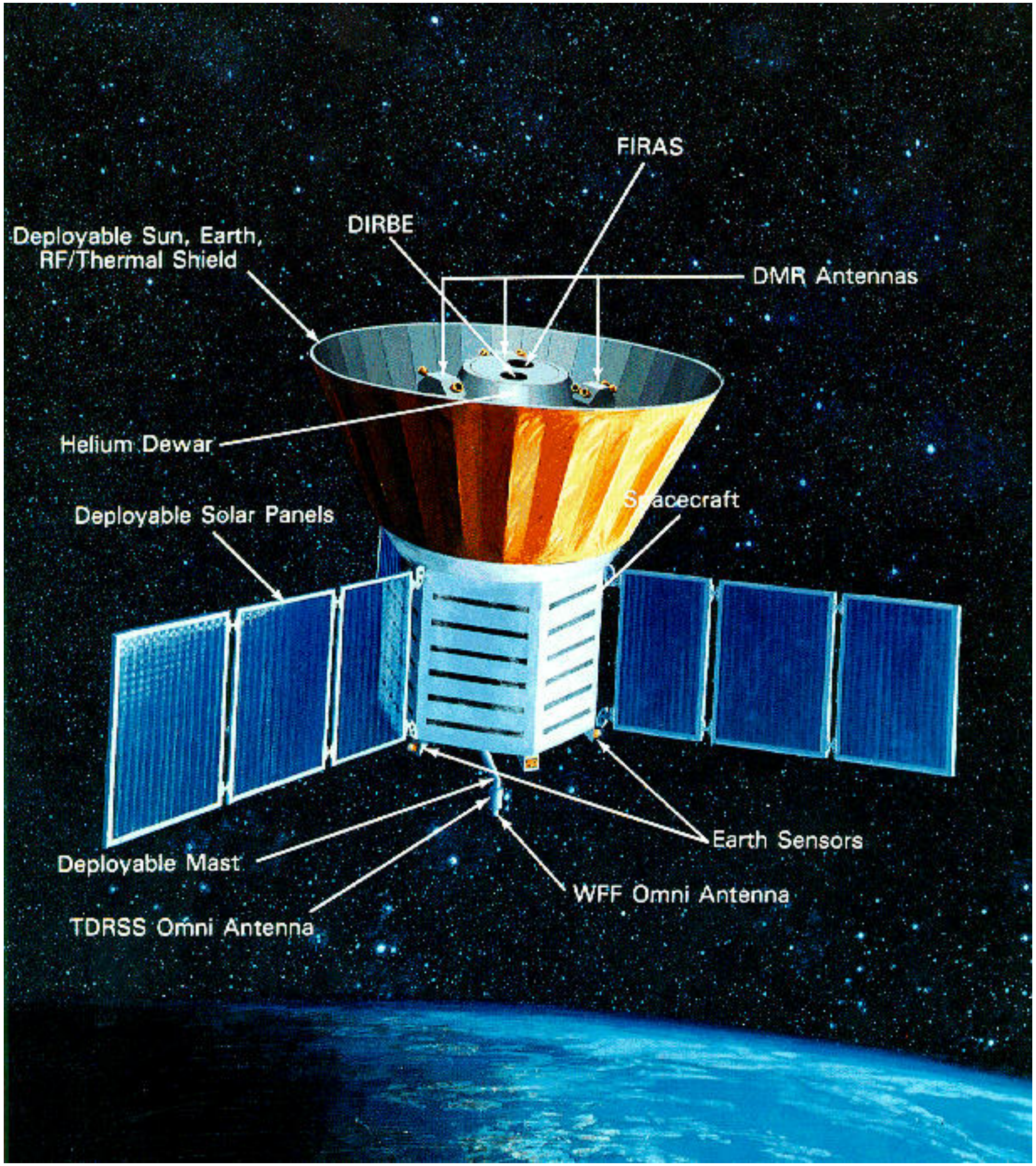
FIRAS
DIRBE
Deployable Sun, Earth,
RF/Thermal Shield
DMR Antennas
Helium Dewar
Spacecraft
Deployable Solar Panels
Earth Sensors
Deployable Mast
WFF Omni Antenna
TDRSS Omni Antenna

COBE results

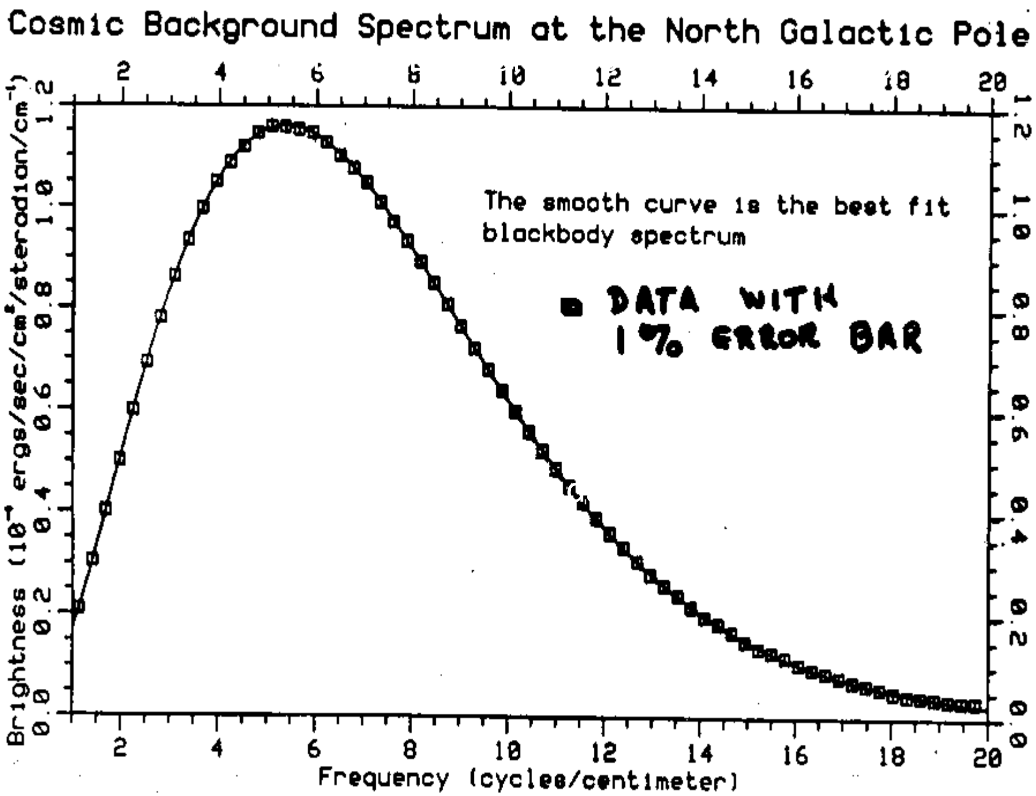

First FIRAS data

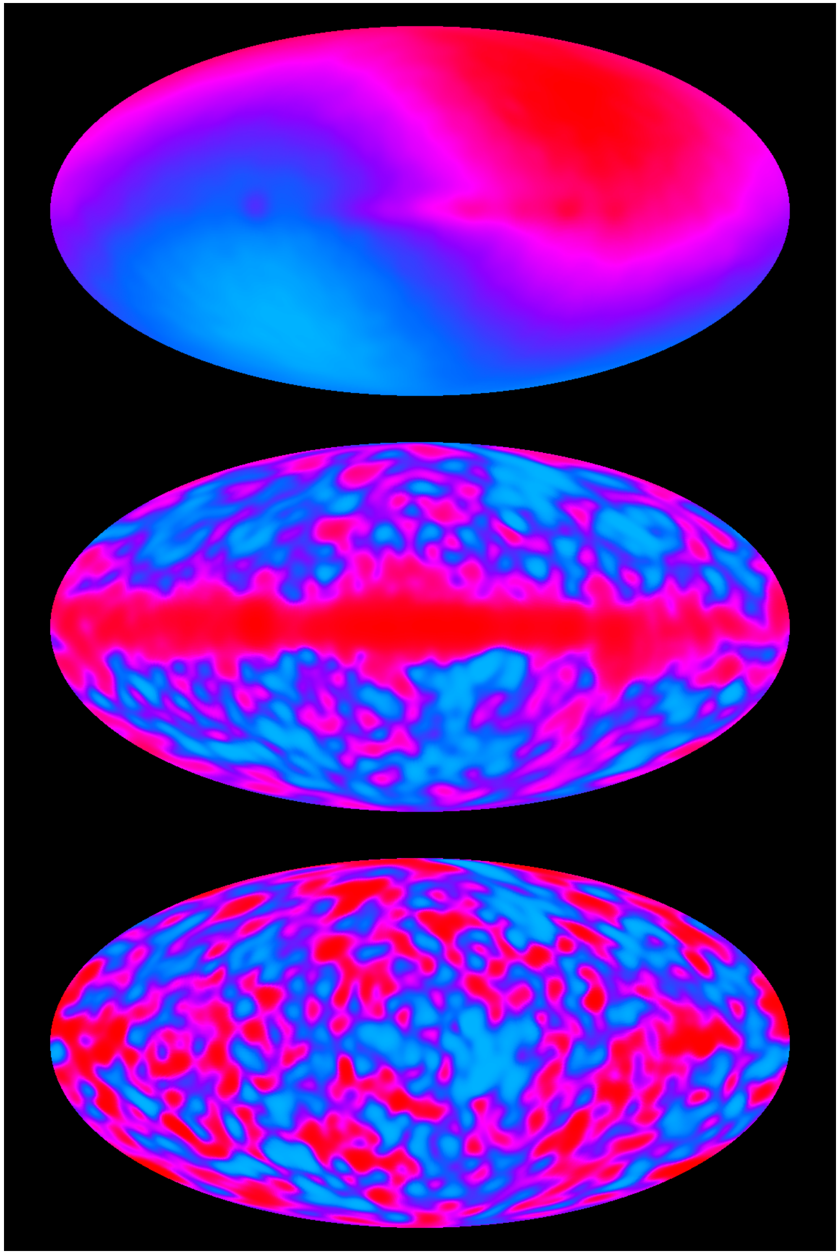

55 and 90 GHz DMR channels

Earth's velocity around sun

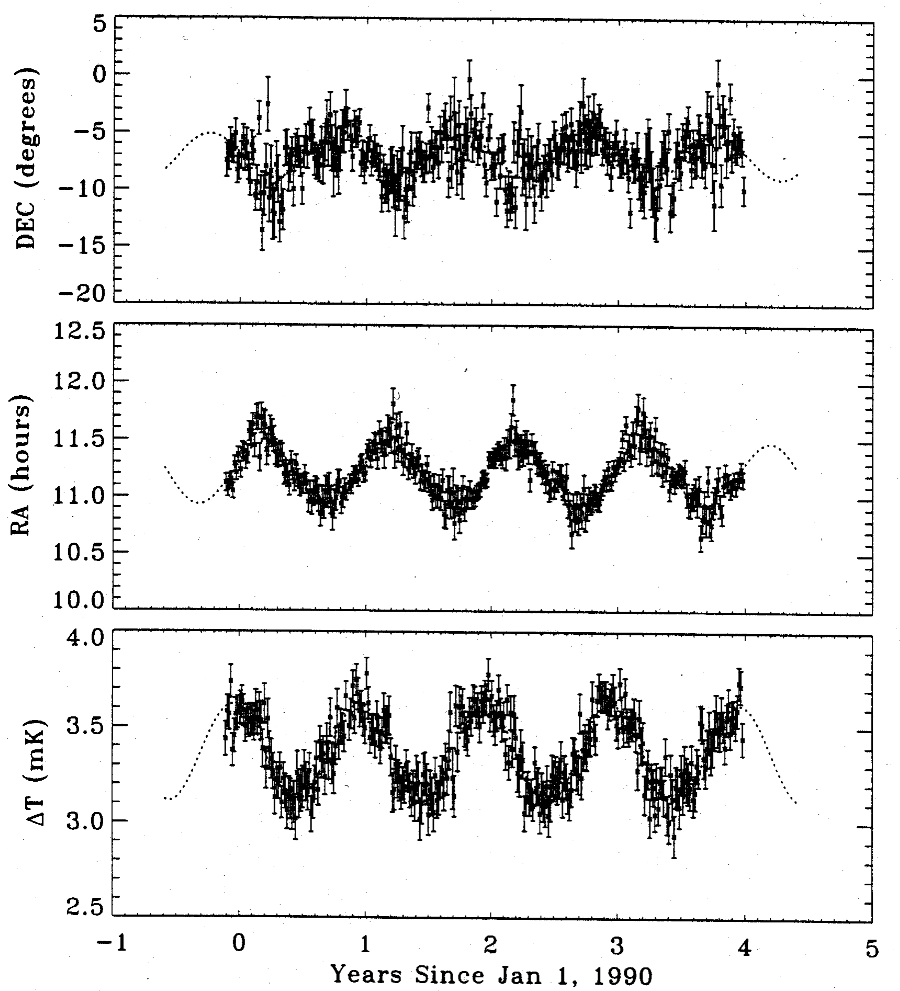

Figure 3: Modulation of the CMB dipole resulting from the Doppler effect of the Earth's orbital motion about the Sun (channel 53B). Each datum represents 5 days. The amplitude of the modulation provides an independent absolute calibration.

Tired Photons: chipping away by collisions Finlay-Freundlich hypothesis

LETTERS TO THE EDITOR

Red-Shifts in the Spectra of Celestial Bodies*

Stars of high surface temperature, that is B-stars ($T \sim 20\,000$°K) and O-stars ($T \sim 30\,000$°K), show a very marked red-shift of their spectral lines. This is especially noticeable in the case of the stars embedded in the Orion Nebula, since in that case it is possible to deduct from the observed red-shifts the red-shift due to the recession of the system as a whole. If one considers these stars, it is found that, relative to the Orion Nebula itself, the B-stars show a systematic red-shift corresponding to a recession velocity of 11·4 km sec^{-1} and a similar discussion of O-stars gives a red-shift corresponding to 17·6 km sec^{-1}.†

In earlier discussions it was suggested that this red-shift might be due to the relativistic gravitational effect. From the known masses and radii of B-stars it follows, however, that the gravitational effect would only lead to red-shifts of the order of 1·2 km sec^{-1}, which are by a factor 10 smaller than the observed red-shifts.

While the observed red-shifts in the case of B- and O-stars are by far larger than the relativistic red shifts, in the case of the sun the situation is just the opposite. In this case most detailed and accurate data are available, but while the theory of relativity predicts a red-shift $\Delta\lambda/\lambda = 2\times10^{-6}$, the red-shift in the centre of the solar disc is only 8×10^{-7}, although the relativistic value is reached, and even surpassed, at the limb. A careful analysis of the red-shift in the solar spectrum shows that it follows the law $\Delta\lambda/\lambda = a + b \sec\theta$, where θ is the angle between the line of sight and the solar radius to the point where the line of sight cuts the solar surface.

It is tempting to try to account for all these red-shifts by one process and we suggest the following formula:

$$\Delta\lambda/\lambda = AT^4 l, \qquad A = 2\times10^{-29}\ \mathrm{cm^{-1}\,deg^{-4}}. \qquad \ldots\ldots(1)$$

In eqn (1) $\Delta\lambda/\lambda$ is the relative red-shift, T the temperature of the radiation field through which the light has passed and l the length of its path through the radiation field. The constant A is chosen in such a way that $\Delta\lambda/\lambda = 3\times10^{-5}$ for $T = 20\,000$°K, $l = 10^7$ cm, which are the values for a B-star. Formula (1) implies that the red-shift is due to a loss of energy in the intense radiation field, perhaps *due to photon–photon interactions.*

It turns out that eqn (1) can well account for most of the observed red-shifts. For the sun we get $\Delta\lambda/\lambda = 2{\cdot}7\times10^{-7}\sec\theta$, while the observed value of b is $3{\cdot}0\times10^{-7}$. The constant term a may be due to a gravitational effect, which in that case would be about five times smaller than the theoretically predicted constant red-shift.‡

In the case of A-stars eqn (1) predicts a red-shift of about 0·6 km sec^{-1}, while the observed red-shifts lie between 0·1 and 0·9 km sec^{-1}. In the case of

* A more detailed account of the subject matter of the present note can be found elsewhere (Freundlich 1954 a, b).

† I would like to express my thanks to T. B. Slebarski for critically discussing the available data.

‡ *It is of interest to note that the red-shift in Sirius B, which can only be due to a gravitational effect, is also about five times smaller than the theoretical value.*

supergiant M-stars T is very small, but their enormous atmospheres—about a thousand times more extensive than the solar atmosphere—lead to expected red-shifts of about 5 km sec^{-1}. It is found that lines formed at the top of the atmosphere are, indeed, displaced by about 5 km sec^{-1} to the violet with respect to lines formed at the bottom of the atmosphere. In the case of Wolf–Rayet stars ($T \gtrsim 40\,000$°K) eqn (1) leads to red-shifts of the order of 100 km sec^{-1}, which also have been observed (Wilson 1949).

Finally, it seems tempting to apply formula (1) to the case of the cosmological red-shift or Hubble effect. In that case $\Delta\lambda/\lambda$ is about 0·0008 for every million parsec ($= 3\times10^{24}$ cm). Using eqn (1) this leads to an intergalactic temperature of about 1·5°K, which does not seem to be an unreasonable value.

The Observatory, University of St. Andrews. E. Finlay-Freundlich.

7th December 1953.

Freundlich, E. F., 1954 a, *Göttinger Nachr.*, No. 7; 1954 b, *Phil. Mag.*, **45**, in the press.
Wilson, O., 1949, *Astrophys. J.*, **109**, 76.

On the Interpretation of Freundlich's Red-Shift Formula

Freundlich (1954) has suggested that his red-shift formula $\Delta\nu/\nu = -AT^4 l$ ($A = 2\times10^{-29}$ cm^{-1} deg^{-4}) may be interpreted as an effect of photon–photon collisions. I have investigated whether this is possible. The first step is to write the equation in a dimensionless form,

$$\frac{\Delta\nu}{\nu} = -C\frac{l}{l_0}\frac{u}{u_0} \qquad \ldots\ldots(1)$$

where $u = aT^4$ ($a = 7{\cdot}66\times10^{-15}$ erg cm^{-3} deg^{-4}) is the radiation density according to Stefan's law. If one takes for l_0 and u_0 the atomic constants

$$\left.\begin{aligned} l_0 &= \frac{\lambda_0}{2\pi} = \frac{\hbar}{mc} \qquad (\lambda_0 = \text{Compton wavelength}) \\ u_0 &= \frac{mc^2}{l_0^3} = \frac{\hbar c}{l_0^4} \qquad (\text{one electron per cube } l_0^3) \end{aligned}\right\} \qquad \ldots\ldots(2)$$

one has

$$l_0 u_0 = \frac{\hbar c}{l_0^3} = 5{\cdot}54\times10^{14}\ \mathrm{erg\,cm^{-2}} \qquad \ldots\ldots(3)$$

and obtains

$$C = \frac{l_0 u_0}{a}A = 1{\cdot}45, \qquad \ldots\ldots(4)$$

a value so near to unity that the assumptions (2) seem to be justified.

A simple analysis of (1) then leads to the result that it can be written in the form

$$\Delta\lambda/\lambda = -\Delta\nu/\nu = CN\lambda_0/\bar{\lambda}, \quad N = ll_0^2 n \qquad \ldots\ldots(5)$$

where n is the number of photons per unit volume and $\bar{\lambda}$ the wavelength corresponding to the mean frequency of the radiation field defined by $u = n\hbar\bar{\omega}$.

Hence the red-shift can be explained as a sequence of N photon–photon collisions with an effective cross section l_0^2, each of which produces a small change in wavelength or frequency

$$\delta\lambda/\lambda = C\lambda_0/\bar{\lambda}, \quad \delta\nu = -C\nu\bar{\nu}/\nu_0. \qquad \ldots\ldots(6)$$

Quantum electrodynamic photon-photon scattering

photon-photon cross section for $\frac{E_\gamma}{m_e c^2} << 1$ in CM system H.Euler (1936)

$$\sigma(\gamma,\gamma) = \frac{1}{\pi^3 450}\alpha^4 \left(\frac{h}{m_e c}\right)^2 \left(\frac{E_\gamma}{m_e c^2}\right)^6 = 1.2x10^{-32}\left(\frac{E_\gamma}{m_e c^2}\right)^6 \mathrm{cm}^2$$

mean free path of a green photon in the 3K cosmic background radiation

$$\lambda = \frac{1}{\sigma(\gamma,\gamma)n_{cmb}} \sim 8x10^{62}\,\mathrm{cm} \sim 8x10^{44}$$ light years

Finlay-Freundlich hypothesis has nothing to do with QED

The interferometric test of Finlay-Freundlich

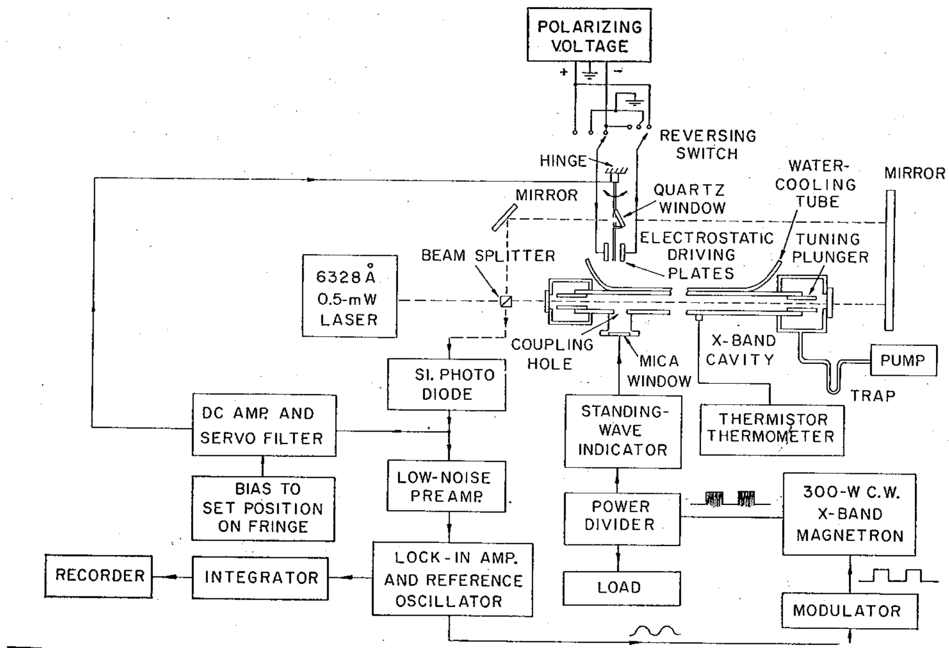

FIG. 1. Block diagram of the apparatus.

FIG. 2. Sample data. The trace on the left shows the lock-in amplifier output signal with pulsed cavity power on and off. The + and − signs refer to the servo polarizing voltage. The trace on the right is the Kerr effect in air when the cavity is brought to atmospheric pressure.

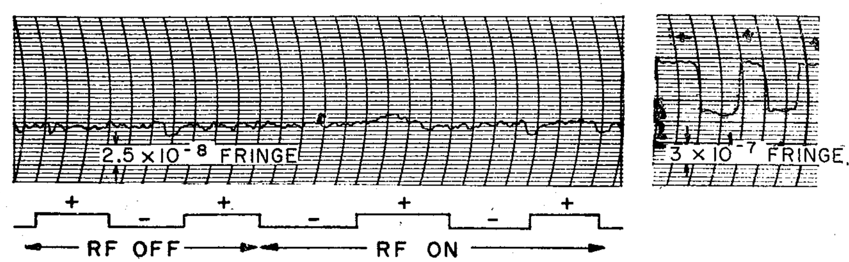

results

G. Blum

$$\frac{\Delta f}{f} = kL$$

$K_{hubble}=8.3\times10^{-29}$ /cm

$K_{experiment}=3.0\times10^{-39}$ /cm assuming scattering varies as number of photons/cc

LIGO@Livingston